



Finite element simulation of cold pilgering of ODS tubes

Esteban Vanegas Márqueza, Katia Mocellin, Louise Toualbi, Yann De Carlan,
Roland E. Logé

► To cite this version:

Esteban Vanegas Márqueza, Katia Mocellin, Louise Toualbi, Yann De Carlan, Roland E. Logé. Finite element simulation of cold pilgering of ODS tubes. SF2M - Société Française de Métallurgie et de Matériaux. Journées Annuelles de la SF2M 2012 - SF2M Annual Meeting 2012, Oct 2012, Paris, France. 2 p., 2012. <hal-00759474>

HAL Id: hal-00759474

<https://hal-mines-paristech.archives-ouvertes.fr/hal-00759474>

Submitted on 30 Nov 2012

HAL is a multi-disciplinary open access archive for the deposit and dissemination of scientific research documents, whether they are published or not. The documents may come from teaching and research institutions in France or abroad, or from public or private research centers.

L'archive ouverte pluridisciplinaire **HAL**, est destinée au dépôt et à la diffusion de documents scientifiques de niveau recherche, publiés ou non, émanant des établissements d'enseignement et de recherche français ou étrangers, des laboratoires publics ou privés.

Finite element simulation of cold pilgering of ODS tubes

E. Vanegas Márquez^a, K. Mocellin^b, L. Toulbi^a, Y. de Carlan^a and R.E. Logé^b

^aCEA/DEN/Service de Recherches Métallurgiques Appliquées 91191 Gif-sur-Yvette, France

^bMines ParisTech, CEMEF - Centre de Mise en Forme des Matériaux, CNRS UMR 7635

BP 207, 1 rue Claude Daunesse 06904 Sophia-Antipolis

Abstract

The oxide dispersion strengthened (ODS) ferritic and martensitic steels are candidate cladding materials for the new fast-neutron sodium-cooled Generation IV reactors. Typically the cladding is cold formed by a sequence of cold pilger rolling passes with intermediate heat treatments. Cracking risk prediction in pilgering is linked to the choice of an appropriate constitutive model for modeling the process. Consequently, this work aims to assess the impact of the constitutive laws on cracking risk development in pilgering conditions.

1. Introduction

Oxide dispersion strengthened (ODS) ferritic/martensitic alloys are promising cladding materials for sodium-cooled fast nuclear reactors intended within Generation IV. This is due to their excellent creep properties and superior irradiation resistance [1], compared to other conventional heat resistant steels such as 9Cr ferritic/martensitic steels and austenitic steels. Excellent creep properties are obtained thanks to the nanometric oxide particles dispersed in the matrix. These nanometric oxides are supposed to be very stable under neutron irradiation and at high temperatures.

ODS materials are obtained by powder metallurgy. Once the powder has been obtained, consolidation of the ODS materials is achieved either by hot extrusion, or by hot isostatic pressing. Subsequently, the cladding is cold formed by a sequence of cold pilgering rolling passes with intermediate heat treatments, for stress relief purposes [2].

The HPTR cold pilgering process is a widespread seamless tube forming operation in which the tube wall thickness and the inner diameter are reduced simultaneously. This technique provides a high forming rate, narrow tolerances and good turnouts. The process uses a reciprocating, or back-and-forth, motion. After each back and forth movement (stroke) of the dies, the raw tube is translated by a small distance and rotated around its axis. A volume element takes several dozens of strokes before deformation is completed. This complex mechanical history may lead to the nucleation of defects in low-cycle fatigue regime [3]. The goal is to build a robust numerical model to describe the mechanical conditions that prevail during a pilgering pass. In this work, the influence of the ferritic ODS constitutive law, on the prediction of defect, is assessed. Consequently deformation path should be identified using a numerical simulation because of the complexity of the kinematics. Moreover the constitutive law must be accurate enough to describe the pilgering mechanical loadings. Comparing with the bibliography

where only monotonic laws are used to simulate in 3D the pilgering process. The full stroke numerical simulation of the cold pilgering process leads to the determination of the strain path undergone by a material point. This task is new comparing to literature.

2. Simulation set up

Optimizing numerically the whole process with a long tube is simply not feasible at the time being, because of the huge computation time involved. Consequently, a *short tube* approach is used. A pilgering pass where deformation is close to 25% is simulated. The tube is turned 39° and moved forward (feed) 1.7 mm after each stroke. A material point takes 120 strokes to pass through the working zone. Initial position of the simulated systems is displayed in Figure 1. Lagrangian numerical sensors have been placed at the mid-length of the tube at different angles.



Figure 1. FEM simulation set-up.

3. Monotonic constitutive model

A standard constitutive model adapted to described monotonic loadings, tensile is used. The elastic-viscoplastic Hansel-Spittel law is chosen, it is given by :

$$\sigma_0(\bar{\epsilon}) = A e^{m_1 T} T^{m_9} \bar{\epsilon}^{m_2} e^{m_4 \bar{\epsilon}} (1 + \bar{\epsilon}^{m_5 T}) e^{m_7 \bar{\epsilon}} \dot{\bar{\epsilon}}^{m_3} \dot{\bar{\epsilon}}^{m_8 T}$$

where $\bar{\epsilon}$ is the equivalent deformation (total strain), $\dot{\bar{\epsilon}}$ the equivalent deformation rate (total strain rate), T is the temperature and A , m_{1-9} are the regression coefficients. A isothermal tensile test is considered, no strain rate effects is assumed: parameters m_3 and m_8 are therefore set to zero.

4. Cyclic elastic-plastic constitutive model

The cyclic deformation induced by cold pilgering is fairly well approximated by a sequence of compression tests

along two perpendicular directions [4]. The constitutive model considered in this study is therefore based on Chaboche for the cyclic behavior, it is denote as *cyclic C/C*. The latter utilizes multi-components forms of kinematic and isotropic hardening variables with non-linear evolutionary rules to describe the hysteresis loops and the transient behavior of the material.

The formulation chosen here is the following [5]. The elastic domain is defined by:

$$f = J_2 \left(\underline{\sigma} - \sum_i \underline{X}_i \right) - \sum_i R_i - \sigma_y \leq 0$$

In the previous equation σ_y is the initial yield surface size. \underline{X} is the kinematic internal stress tensor and R is the isotropic hardening. The formulation of the kinematic hardening tensor is based on the non-linear Chaboche kinematic model.

5. Damage

The criterion introduced by Latham and Cockroft and used in this work establishes the damage function from the principal stresses. This damage criterion was already used for VMR cold pilgering (e.g. [6]) and seems to be a good indicator to predict defects frequency. Compressive stresses have a negligible effect on damage compared with tensile ones; so in its original version this criterion does not take them into account. The classical damage function used in [6] is the sum of the product of the maximum tensile stress at each stroke. This function represents an indicator of the material state.

Considering the HPTR cold pilgering process, and the experimental evidence of longs cracks along the rolling axis, it is proposed to consider each strain increments in all directions ($\Delta \epsilon_i$, $i = rr, \theta\theta, zz, r\theta, \theta z, rz$). Similarly, the expression of the maximal stress is modified in order to consider only positive stress components. Finally, authors have shown that damage occurs for mechanical states where the triaxiality is higher than -1/3. A modified cumulative damage function (Lat&Co) is then proposed:

$$Lat \& Co_{(i)} = \sum_{\substack{\text{Stroke} \\ \text{triaxiality} \geq -1/3}} \sigma_i^+ * \Delta \epsilon_i^+$$

Where $i = rr, \theta\theta, zz, r\theta, \theta z, rz$, $\sigma_i^+ = \max(0, \sigma_i)$, $\text{triaxiality} = \sigma_H / \sigma_{eq}$ with σ_H the hydrostatic pressure and σ_{eq} the equivalent stress. Thus, it is possible to obtain a cumulative damage field in each mechanical solicitation direction.

Longitudinal damage function is maximal when comparing with other directions (not showed here). Figure 2 shows the sensor (located at mi-length and mid-thickness). Longitudinal damage function evolution for each constitutive law. Longitudinal damage is highest for the

cyclic C/C behavior law. Even with the huge stress values predicted by monotonic laws; the longitudinal damage value is lower than the cyclic law. Hence, when the cyclic constitutive law is taken into account, the material follows more *daming* situations.

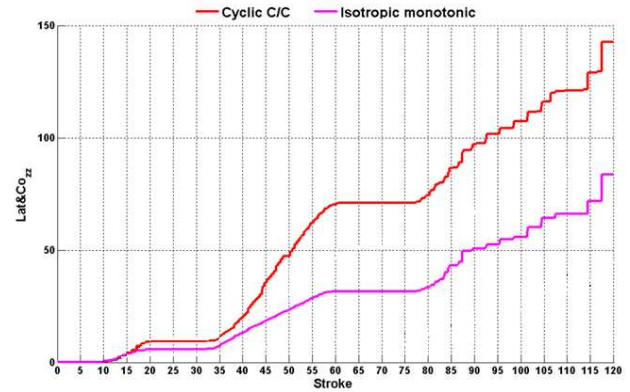


Figure 2. Longitudinal damage function history in sensor S2 (in MPa).

Looking at Figure 2 and considering the *cyclic C/C* behavior law, damage function increases dramatically between strokes 35-55 and 80-110 for the longitudinal component. Monotonic behavior law also leads to an increase, but with lower intensity.

6. Conclusions

Accurate modeling of the material constitutive behavior is one of the most important features needed in order to simulate the process properly. Full numerical simulations considering the monotonic and cyclic constitutive behavior of ODS steels were carried out. A systematic analysis of all strokes has helped defining which stroke could contribute mainly to the oligocyclic fatigue of the material. Future work will include a numerical simulation of ODS tubes cold pilgering considering anisotropic-cyclic constitutive behavior. The influence of this feature on the mechanical history undergone by a material point during the process will be assessed.

7. References

- [1] Y. de Carlan *et al.*, J. Nucl. Mater. 386-388 (2009) 430-432.
- [2] L. Toulbi *et al.*, Proceedings of DIANA I workshop "Dispersion Strengthened steels for advanced nuclear applications", Aussois (France) April 4-8, 2011, J. Nucl. Mater.
- [3] P. Montmitonnet *et al.*, J. Mater. Proc. Tech. 125-126 (2002) 814-820.
- [4] E. Vanegas-Marquez *et al.*, J. Nucl. Mater. 420 (2012) 479-490.
- [5] J.-L. Chaboche, Int. J. Sol. Struc. 34 (1997) 2239-2354.
- [6] E. Girard *et al.*, J. Nucl. Mater. 294 (2001) 330-338.